Numerical modeling of diffusive heat transport across magnetic islands and highly stochastic layers

M. Hölzl, S. Günter, Q. Yu, and K. Lackner

Max-Planck-Institut für Plasmaphysik, EURATOM Association, 85748 Garching, Germany

Abstract

Diffusive heat transport across magnetic islands and highly stochastic layers is studied numerically for realistic values of $\chi_{||}/\chi_{\perp}$ in cylindrical geometry, where $\chi_{||}$ denotes the heat diffusion coefficient parallel and $\chi_{\perp}$ the one perpendicular to the magnetic field lines. The computations are performed with a second order finite difference scheme, for which the numerical errors are independent from the value of $\chi_{||}/\chi_{\perp}$ [S. Günter *et. al.*, J. Comput. Phys. **209**, 354 (2005)]. Sufficient spatial resolution is ensured by using an unsheared helical coordinate system. The heat flux around magnetic islands as well as the effective radial heat diffusivity χ_r are examined and compared to analytical theory. The temperature perturbations caused by magnetic islands and the resulting bootstrap current perturbations essential for the stability of neoclassical tearing modes (NTMs) are analyzed and compared to analytical predictions [R. Fitzpatrick, Phys. Plasmas **2**, 825 (1995)]. Agreement is found in the "small" and "large" island limits,

but an enhanced NTM drive is observed in between. A correction factor that can reproduce the numerical results very well is presented. For a highly stochastic layer, produced by five strongly overlapping islands, the radial heat diffusivity χ_r is determined and compared to several analytical theories.

I. Introduction

Diffusive heat transport in strongly magnetized plasmas is characterized by a large anisotropy of the heat diffusion tensor, which results from the electron mobility being much higher parallel to the magnetic field lines than perpendicular to them. In state-of-the-art fusion experiments, the ratio between the parallel heat diffusion coefficient $\chi_{||}$ and the perpendicular one, $\chi_{\perp}$, reaches values up to 10^{11} (see Ref. [1]). In this work, the heat transport across magnetic islands and highly stochastic layers is studied for realistic values of $\chi_{||}/\chi_{\perp}$ in an equilibrium with a simplified geometry (circular cross-section, large aspect ratio).

In unperturbed equilibria with nested magnetic surfaces, the radial heat transport is exclusively conducted by perpendicular transport. But in the presence of magnetic islands, nested island magnetic surfaces exist [1]. Radial heat transport increases as it gains a parallel contribution, and the temperature profile partly flattens, reducing the overall energy confinement [1, 2]. The effect of such temperature perturbations on the neoclassical bootstrap current can lead to further island growth (neoclassical tearing modes, NTMs) and thus to a further degradation of energy confinement [1, 3–5]. To quantify this effect, knowledge of the exact temperature distribution is required, which we gain from the steady state heat diffusion equation.

Stochastic fields are used at the plasma edge in some tokamak experiments to achieve a more evenly distributed energy load on the walls and possibly to suppress edge localized modes

(ELMs) [6, 7]. The increase of the radial heat transport in a highly stochastic layer is investigated and the results are compared to analytical predictions [2, 8–12].

Physical and numerical details of our model are presented in Section II. All single island related results can be found in Section III. Our results for the heat diffusion across highly stochastic layers are presented in Section IV.

II. Model

A. Physical model

In this work, we limit ourselves to a plasma equilibrium with a circular cross section and a large aspect ratio ("$2\pi R_0$ periodic cylinder"). The minor radius is labeled a, the local minor radius r, the major radius R_0, the poloidal angle θ, and the "toroidal angle" ϕ. In this geometry, the steady state heat diffusion equation

$$\nabla \cdot \vec{q} = P, \tag{1}$$

is solved, where P is the heat source and

$$\vec{q} = \vec{q}_{||} + \vec{q}_{\perp} = -n\chi_{||}\nabla_{||}T - n\chi_{\perp}\nabla_{\perp}T \tag{2}$$

is the heat flux density consisting of the contributions parallel and perpendicular to the magnetic field lines. The particle density is denoted n and assumed to be constant, the magnetic field

direction is labeled $\hat{b} = \vec{B}/B$ and the parallel and perpendicular temperature gradients are defined as $\nabla_{||}T = \hat{b}(\hat{b}\cdot\nabla T)$ and $\nabla_{\perp}T = (\nabla - \nabla_{||})T$. We assume the heat diffusion coefficients $\chi_{||}$ and $\chi_{\perp}$ to be constant.

The boundary conditions $T(r = a) = 0$ and $\lim_{r\to 0} dT/dr = 0$, where a denotes the minor radius, are applied. The toroidal magnetic field component B_ϕ is taken to be constant. The poloidal magnetic field component B_θ can be expressed in terms of B_ϕ and the safety factor $q = rB_\phi/R_0B_\theta$, for which the analytical expression $q(r) = 0.9[1 + (r/0.48a)^4]^{0.5}$ is used, yielding to $q(0) = 0.9$ and $q(a) = 4$. To avoid energy sources within the island regions, central heating inside $r = 0.2a$ is applied with $P(r) = P_0[1-3(r/0.2a)^2+2(r/0.2a)^3]$ and $P(r) \equiv 0$ for $r \geq 0.2a$. Here, the amplitude P_0 is usually chosen such that the unperturbed temperature at $r = 0$ is normalized to unity.

For the poloidal flux of magnetic perturbations, $\Psi_{pert} = \Psi_{pert,0} \cdot r^2(1 - r^2)^2 \cos(m\theta - n\phi)$ is used, where m and n denote the poloidal and toroidal mode numbers of the perturbation, as it has been done in previous work [2]. This model is well-suited to study magnetic islands although it is not very close to the solution of the tearing mode equation (see Ref. [13]) in general. A possible shift of the plasma center due to $m = 1$ magnetic perturbations is not considered.

B. Mathematical and numerical model

For this work, a second order finite difference scheme is applied in radial and poloidal directions. The scheme developed in [14] conserves the self-adjointness of the parallel heat diffusion operator and uses staggered grids for the heat fluxes and temperatures. By this means, numerical pollution of the perpendicular heat flux by parallel heat transport can be avoided, even if no coordinate line is parallel to the magnetic field lines. The scheme has recently been extended to finite element descriptions and higher order finite differences [15].

To ensure sufficient spatial resolution, the coordinate system is approximately aligned to the magnetic perturbations by chosing a helicial coordinate system with constant rational helicity $q_c = m_c/n_c$. It is derived from the cylindrical coordinate system by the transformation $\theta^* = \theta - \phi/q_c$ and becomes cylindrical in the limit $1/q_c = 0$. The rationality of q_c causes coordinate lines to close after m_c toroidal turns, which allows for a Fourier decomposition in toroidal direction. The Fourier cutoff is performed at a specific order of the heat flux instead of the temperature to avoid unphysical parallel temperature gradients [14]. The solution of the system of equations is carried out with a double precision sparse matrix solver package called WSMP [16].

For single island cases, the helicity q_c of the coordinate system can be set equal to the helicity $q = m/n$ of the magnetic island, which reduces the problem to two dimensions. For

stochastic cases, a reduction of the problem to two dimensions is not possible. It will be shown in Section III that the numerical errors are already reduced if the coordinate system is only approximately aligned to the magnetic perturbations, as this decreases the temperature gradients along the coordinate lines. Therefore, the computational effort and the numerical errors can be significantly reduced by taking q_c similar to the helicities m_i/n_i of the magnetic perturbations.

III. Magnetic islands

As discussed by Fitzpatrick, the heat flux across magnetic islands is goverened by a competition between parallel and perpendicular contributions and depends only on the ratio between the island width w (largest radial extent of the island separatrix) and the scale island width $w_c = r_s(\chi_{||}/\chi_\perp)^{-1/4}\sqrt{8/\epsilon_s s_s n}$ [1]. Here, r_s denotes the minor radius of the resonant surface, $\epsilon_s = r_s/R_0$ the local inverse aspect ratio, and $s_s = [(r/q)\cdot\partial q/\partial r]_{r_s}$ the local magnetic shear at the resonant surface. For $w = w_c$, the parallel and perpendicular contributions to the radial heat transport are approximately equal.

As mentioned earlier, numerical errors can be reduced by an approximate alignment of the coordinate helicity to the helicity of the perturbations. For a $4/3$ island case ($r_s = 0.502a$, $w = 0.068a$, $\chi_{||}/\chi_\perp = 10^7$, $w/w_c = 1.9$), this is demonstrated in Figure 1, which shows the relative errors $\Delta_{4/3} = |T_{4/3} - T_{4/3,ref}|/T_{4/3,ref}$ of the first temperature harmonic $T_{4/3}$ as

a function of the alignment measure $\xi = |q_c^{-1} - q^{-1}|$, where $q = 4/3$ is the helicity of the magnetic perturbation and the helicity $q_c = m_c/n_c$ of the coordinate system is varied. The errors are computed at the resonant surface for code runs with four toroidal Fourier modes. Results for 600 radial and 160 poloidal grid points resp. 300 radial and 80 poloidal grid points are shown. The reference run was performed in a $q_c = 4/3$ coordinate system with 6000 radial and 2400 poloidal grid points. It can be seen, that the numerical errors are the smaller, the better the alignment.

A. Island heat flux density

Fig. 2 shows plots of the radial and poloidal heat flux density around a $4/3$ magnetic island with an island width of $0.068a$ for different values of $\chi_{||}/\chi_{\perp}$. For small w/w_c, the heat flux is almost unaffected by the island (Fig. 2 a). For $w/w_c \gtrsim 2$, heat is transported around the island within a heat conduction layer, which is located mainly inside the island separatrix (Fig. 2 b–d). The heat conduction layer, marked in the figures with a grey background, is the region with significant parallel transport around the island ($q_{||,r} > 0$ and $|r\vec{q}_{||}| > Max|r\vec{q}_{\perp}|/3$, where the maximum is taken over the whole plasma region). Most heat crosses the resonant surface close to the island x-point.

Perpendicular transport from the plasma center towards the island heat conduction layer across flux surfaces is more efficient in the o-point region than in the x-point region, as the

distance between the flux surfaces is smaller there. The fast parallel transport consequently redistributes heat flux within the flux surfaces from the x-point region to the o-point region. This can be seen from Fig. 3, where $\vec{q}_{||}$ is plotted only outside the heat conduction layer to make this relatively small effect visible. As the parallel transport outside the heat conduction layer has a radial component directed towards the plasma center (Fig. 3), the total outward radial heat transport is reduced there. Similar arguments hold for the transport from the heat conduction layer towards the plasma edge.

B. Effective radial heat diffusivity

The radial heat transport across magnetic islands can be measured by the poloidally and toroidally averaged effective radial heat diffusivity coefficient χ_r. It is determined from the $0/0$ component of the steady state heat diffusion equation $\nabla \cdot \vec{q}_{0/0}(r) = P(r)$ where $q_{r,0/0}(r) = -n\chi_r(r)T'_{0,0}(r)$. After the integration $\int_r^a dr r \ldots$ it is found to be

$$\chi_r(r) = \frac{a\,\chi_\perp(a)\,T'_{0,0}(a) + n^{-1}\int_r^a dr\; rP(r)}{r\,T'_{0,0}(r)}. \tag{3}$$

where $\chi_r(a) \approx \chi_\perp(a)$ has been made use of. The effective radial heat diffusivity coefficient χ_r is strongly increased in the island region compared to the perpendicular heat diffusivity coefficient $\chi_\perp$ as seen from Fig. 4, where $\chi_\perp/\chi_r$ is plotted. Equal contributions from parallel and perpendicular heat transport, i.e., $\chi_r \approx 2\chi_\perp$, are found at the resonant surface for $w/w_c = 1.8$. For comparison, the profiles of χ_r according to an analytical theory by Yu, derived for

$w/w_c \ll 1$, are also plotted [2]. For w/w_c of about unity, the analytical theory is in very good agreement with the numerical results. Even for $w/w_c = 1.8$, reasonable agreement is observed although the formula has been derived assuming $w/w_c \ll 1$. For still higher values of w/w_c, no useful results can be obtained from it anymore.

As shown in Subsect. A, parallel heat diffusion slightly reduces the overall radial heat transport outside the heat conduction layer. Therefore, the radial heat diffusivity χ_r can be expected to be smaller than $\chi_\perp$, there. This effect can indeed be seen from Fig. 4.

In Fig. 5, the dependence of χ_r on w/w_c is examined at the resonant surfaces of different island cases, showing that χ_r depends on w/w_c only. Two different regimes can be identified: $\kappa = (\chi_r - \chi_\perp)/\chi_\perp \propto [w/w_c]^4$ for small w/w_c and $\kappa \propto [w/w_c]^2$ for large w/w_c. They are separated by a transition region between $w/w_c \approx 1$ and 4.5. These results are in good agreement with previous analytical and numerical work [1, 2].

C. Neoclassical tearing modes

The increased radial heat diffusivity brings about a flattening of the temperature profile in the island region, which perturbs the bootstrap current. This, in turn, leads to a neoclassical contribution to the island growth rate, which is positive for conventional tokamak plasma profiles [1]. Islands destabilized by this contribution are called neoclassical tearing modes (NTMs). The island growth rate is $dw/dt \propto \Delta' + \Delta_{bs}$, where Δ' is the classical tearing stability index and Δ_{bs}

is the contribution from the temperature perturbations. Fitzpatrick derived analytical expressions for the island drive in the limits of small and large w/w_c from his analytical results for the temperature perturbations and performed an analytical matching between these two limits [1]:

$$\Delta_{bs} = 4.63 \frac{\mu_0 \, q_s^3 \, p_s'}{B_z^2 \, \epsilon_s^{3/2} \, q_s'} \cdot \frac{2 r_s \, w}{w^2 + w_d^2}. \tag{4}$$

Here, $w_d \approx 1.8 w_c$, the toroidal field strength is denoted B_z, the unperturbed pressure gradient at the resonant surface is denoted $p_s' = n T_s'$, the resonant value of the safety factor is denoted q_s, and its gradient q_s'.

We compute Δ_{bs} analogical to Fitzpatrick for three different $3/2$ and one $4/3$ island case, but from the numerically obtained temperature perturbations. In Fig. 6, we plot results for $\Delta_{bs,norm} = (w \, \sqrt{r_s} \, q_s'/T_s' \, q_s^3) \cdot \Delta_{bs}$. For each curve, w_c is varied by changing the value of $\chi_{||}/\chi_{\perp}$. In the small and large island limits, the numerical results agree very well with the analytical predictions. For intermediate ratios of w/w_c, however, Eq. (4) underestimates the island drive significantly. We therefore suggest to change Eq. (4) by multiplying it by the factor

$$\left(1 + \frac{2.2}{(w/w_d)^2 + 3 w_d/w}\right), \tag{5}$$

which takes values in the range between 1 and 1.56. In Fig. 6, very good agreement between the numerical results and the corrected formula is observed for all considered cases. As the correction factor approaches unity for $w/w_d \to 0$ and $w/w_d \to \infty$, the corrected formula fulfills the same analytical small and large island limits as Eq. (4). The maximum with respect

to w (while w_d is kept constant) of Eq. (4) is located at $w = w_d$. The correction factor changes this only slightly to $w = 1.056 w_d$. With respect to w_d (while w is kept constant), the corrected formula has a maximum at $w_d = 0.461 w$ (see Fig. 6), that is absent in Eq. (4).

IV. Highly stochastic layers

For the heat diffusion across highly stochastic layers, extensive analytical work has been done, e.g. by Rechester and Rosenbluth [8], Kadomtsev and Pogutse [10], Stix [9], and Krommes et. al. [11]. A comprehensive review was written by Liewer [12].

A. Analytical theory

Krommes et. al. identified three different subregimes of the collisional regime, where the fluid picture used in this work is valid. They are separated by the ordering of the characteristic electron diffusion times

$$\tau_{||} = L_0^2/\chi_{||} \tag{6}$$

$$\tau_k = L_k^2/\chi_{||} \tag{7}$$

$$\tau_\perp = 1/(k_\perp^2 \chi_\perp) \tag{8}$$

With decreasing collisionality, the regimes are called fluid regime ($\tau_\perp < \tau_{||} < \tau_k$), Kadomtsev-Pogutse regime ($\tau_{||} < \tau_\perp < \tau_k$), and Rechester-Rosenbluth regime ($\tau_{||} < \tau_k < \tau_\perp$). The

diffusion times correspond to the characteristic length scales L_0, L_k and $1/k_\perp$, which are

$$L_0 \approx qR_0, \qquad \text{(quasi-linear autocorrelation length)} \tag{9}$$

$$L_k \approx \left[L_s^2/(k_\perp^2 D_M)\right]^{1/3}, \qquad \text{(Kolmogorov length)} \tag{10}$$

$$D_M = L_0 \sum_{\mathrm{m,n}} \left(B_{r,m/n}/B_{\phi,0}\right)^2, \qquad \text{(magnetic diffusion coefficient)} \tag{11}$$

$$L_s = Rq^2/(rq'), \qquad \text{(magnetic shear length)} \tag{12}$$

$$1/k_\perp \approx r/m. \qquad \text{(characteristic perpendicular wave length)} \tag{13}$$

Here, the radial component of the m/n magnetic perturbation $B_{r,m/n}$, the perpendicular wave vector of the perturbations $k_\perp \approx m/r$, the safety factor q and its radial derivative q' were used. The sum in Eq. (11) must be carried out over all locally resonant m/n magnetic perturbations. The increase χ_r^+ of the radial heat diffusivity $\chi_r = \chi_\perp + \chi_r^+$ in these subregimes is

$$\chi_{r,fl}^+ = D_M \chi_{||}/L_0, \qquad \text{(fluid regime)} \tag{14}$$

$$\chi_{r,KP}^+ = D_M (\chi_\perp \chi_{||})^{1/2} k_\perp, \qquad \text{(Kadomtsev-Pogutse regime)} \tag{15}$$

$$\chi_{r,RR}^+ = D_M \chi_{||}/L_k. \qquad \text{(Rechester-Rosenbluth regime)} \tag{16}$$

In the limit of small w/w_c, Yu recently derived an analytical expression which corrects the fluid regime results by about a factor of $1/2$ for the case considered in the following [2].

B. Numerical examination

We now examine the heat diffusion across a highly stochastic layer numerically and compare our results to the analytical predictions introduced in Subsec. A. The stochastic layer is produced by five magnetic perturbations ($i = 1 \ldots 5$) with the following helicities, island widths and resonant surfaces:

$$q_i = \frac{24}{23}, \frac{25}{24}, \frac{26}{25}, \frac{27}{26}, \frac{28}{27},$$

$$w_i = 0.01876a, 0.01841a, 0.01808a, 0.01777a, 0.01747a,$$

$$r_{s,i} = 0.36767a, 0.36642a, 0.36526a, 0.36418a, 0.36317a.$$

A Poincaré plot of the resulting magnetic configuration is shown in Fig. 7. The commonly used stochasticity parameter, defined between two magnetic perturbations i and j as $s_{i,j} = (w_i + w_j)/2|r_{s,i} - r_{s,j}|$, measures the island overlap and takes values between 4 and 17.5. We define a "total stochasticity" $s = \sum_{i \neq 3} s_{i,3} = 48.5$ to characterize the stochasticity with a single value. Our computations are carried out in a $q_c = 26/25$ helical coordinate system.

Fig. 8 shows that χ_r is increased over the whole ergodic layer. The positions of the rational surfaces are indicated. At the edge of the layer, χ_r is slightly smaller than $\chi_\perp$ for similar reasons as for single islands (see Subsec. III.A and B). In Fig. 9, the dependence of χ_r on $\chi_{||}/\chi_\perp$ is shown at the middle resonant surface $r = r_{s,26/25}$. For small and large values of $\chi_{||}/\chi_\perp$ a linear dependence $\kappa = (\chi_r - \chi_\perp)/\chi_\perp \propto \chi_{||}$ can be seen, while for intermediate

values of $\chi_{||}/\chi_{\perp} \approx 3 \cdot 10^5 \ldots 10^9$ a reduced slope is found in the log-log plot. Basically, these are similar dependencies as predicted by the analytical expressions given in Eqs. (14–16), which are also plotted in Fig. 9. There are, however, two major differences: First, the ranges of validity of the regimes do not coincide. The regime boundaries found numerically are at significantly higher ratios of $\chi_{||}/\chi_{\perp}$ than the analytically predicted ones. Secondly, the analytically predicted values are larger than the numerical results by a factor of roughly two. For the fluid regime, this is not surprising, as the more recent analytical derivation by Yu corrects the fluid regime just by this factor of two. Perfect agreement is found for $w \ll w_c$ (i.e. $\chi_{||}/\chi_{\perp} \ll 6 \cdot 10^6$ for our case), when this correction is applied.

For the Rechester-Rosenbluth regime, an exponential field line diffusion has been assumed by the original authors [8]. Rover et. al., however, performed numerical examinations and concluded that the field line diffusion is substantially different from an exponential behavior [17]. This might well be the reason for the observed deviations between the numerical results and the analytical predictions.

V. Conclusion

With the combination of a 2D finite difference scheme and a Fourier expansion in the third direction, heat diffusion across magnetic islands and highly stochastic layers is studied numer-

ically. An unsheared helical coordinate system is used, which allows to reduce single magnetic island cases to two dimensional problems. Due to the fast parallel transport around the island, the effective radial heat diffusivity χ_r is increased and the corresponding heat conduction layer is located mainly inside the island. Outside the heat conduction layer, however, the parallel transport is oriented opposite to its direction inside the layer and has a small radial contribution directed towards the plasma center. This way, χ_r is slightly smaller than $\chi_\perp$ outside the heat conduction layer of magnetic islands. For the radial profile of χ_r, it is demonstrated that the expression recently derived by Yu for small w/w_c (see Ref. [2]) is valid for w/w_c up to order unity. The effect of temperature perturbations on the stability of NTMs is examined and agreement with the analytical limits for small and large w/w_c is found. The widely used analytical matching between these two limits [1], however, has been shown to underestimate the island growth rate for medium values of w/w_c significantly. We present a correction factor such that the numerical results are reproduced very well.

Heat transport in highly ergodized regions is investigated for an example of five overlapping magnetic islands. In the numerical results for the effective radial heat diffusivity χ_r, good agreement with the qualitative behaviour predicted by Krommes and others is observed for the present case [8–12]. The regions of validity of the regimes, however, do not coincide and the absolute values differ by about a factor of two. In the limit of small w/w_c the analytical theory has recently been corrected by Yu [2]. With this new formula, almost perfect agreement is

found.

VI. Acknowledgements

The authors would like to thank Dr. Erika Strumberger and Dr. Mario Sempf for helpful discussions.

References

[1] R. Fitzpatrick. Phys. Plasmas **2**, 825 (1995).

[2] Q. Yu. Phys. Plamas **13**, 062310 (2006).

[3] R. Carrera, R. D. Hazeltine, and M. Kotschenreuther. Phys. Fluids **29**, 899 (1986).

[4] C. C. Hegna and J. D. Callen. Phys. Fluids B **4**, 1855 (1992).

[5] H. Zohm, G. Gantenbein, A. Gude, S. Günter, *et al.*. Nucl. Fusion **41**, 197 (2001).

[6] M. Lehnen, S. Abdullaev, W. Biel, S. Brezinsek, *et al.*. J. Nucl. Mater. **337–339**, 171 (2005).

[7] T. Evans, R. Moyer, J. Watkins, P. Thomas, *et al.*. J. Nucl. Mater. **337–339**, 691 (2005).

[8] A. B. Rechester and M. N. Rosenbluth. Phys. Rev. Lett. **40**, 38 (1978).

[9] T. H. Stix. Nucl. Fusion **18**, 353 (1978).

[10] B. B. Kadomtsev and O. P. Pogutse. Plasma Physics and Controlled Nuclear Fusion Research, Proceedings of the 7th International Conference, Innsbruck 1978. (International Atomic Energy Agency, Vienna, 1979), Vol. 1, p. 649.

[11] J. A. Krommes, C. Oberman, and R. G. Kleva. Journal of plasma physics **30**, 11 (1983).

[12] P. C. Liewer. Nuclear Fusion **25**, 543 (1985).

[13] D. Biskamp. Nonlinear Magnetohydrodynamics (Camebridge University Press, Cambebridge, 1993), pp. 73–77.

[14] S. Günter, Q. Yu, J. Krüger, and K. Lackner. J. Comput. Phys. **209**, 354 (2005).

[15] S. Günter, K. Lackner, and C. Tichmann. Finite Element and Higher order Difference Formulations for Modelling Heat Transport in Magnetised Plasmas, submitted to J. Comput. Phys.

[16] A. Gupta and M. Joshi. WSMP: Watson Sparse Matrix Package, Part II – direct solution of general sparse systems (2000). IBM T. J. Watson Research Center, 1101 Kitchawan Road, Yorktown Heights, NY 10598x.

[17] M. Rover, A. M. R. Schilham, A. Montvai, and N. J. L. Cardozo. Phys. Plasmas **6**, 2443 (1999).

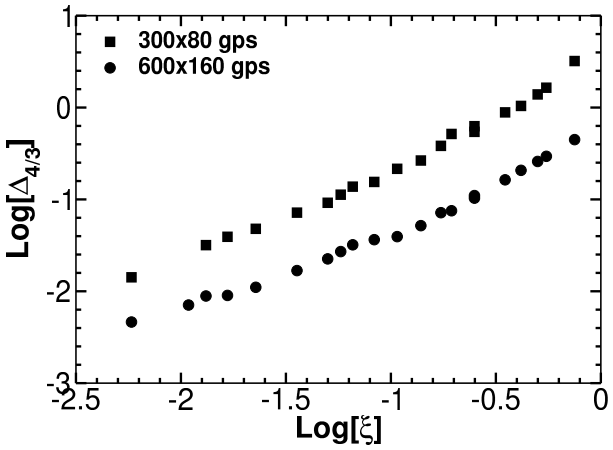

Figure 1: Relative errors in $T_{4/3}$ at the resonant surface for a single $4/3$ island case versus the coordinate alignment measure $\xi = |q_c^{-1} - q^{-1}|$. Approximate alignment of the coordinate system to the helicity of the perturbation significantly reduces numerical errors.

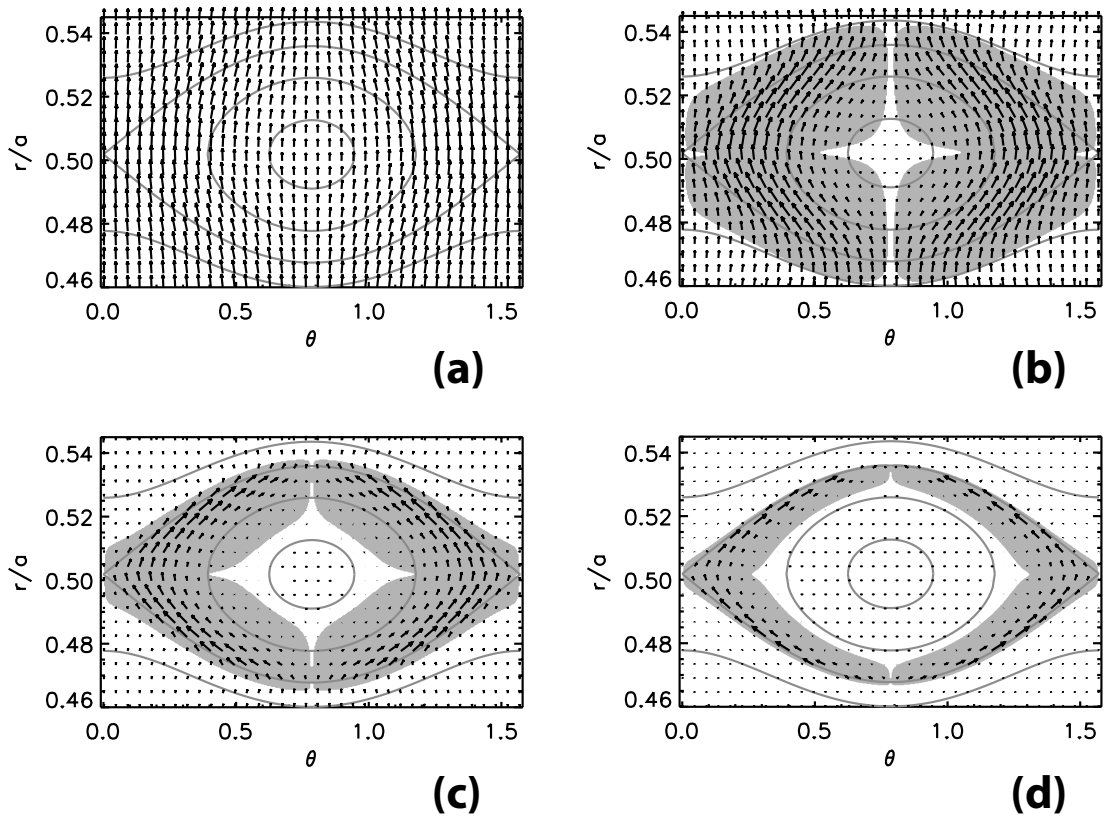

Figure 2: Plots of the heat flux density around a $4/3$ magnetic island with $w = 0.068a$. For $w/w_c \gtrsim 2$, most heat is transported around the island in a heat conduction layer (grey background). Vector lengths are normalized by different factors ν. **(a)** $\chi_{||}/\chi_{\perp} = 10^6$, $w/w_c = 1.1$, $\nu = 1$, **(b)** $\chi_{||}/\chi_{\perp} = 10^7$, $w/w_c = 1.9$, $\nu = 0.24$, **(c)** $\chi_{||}/\chi_{\perp} = 10^8$, $w/w_c = 3.4$, $\nu = 0.074$, and **(d)** $\chi_{||}/\chi_{\perp} = 10^9$, $w/w_c = 6.0$, $\nu = 0.023$.

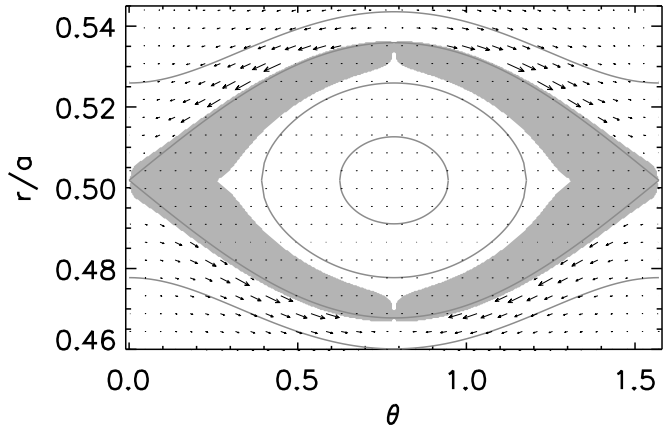

Figure 3: Parallel heat flux density plotted only outside the heat conduction layer for the same case as in Fig. 2 d). A radial contribution directed towards the plasma center is observed.

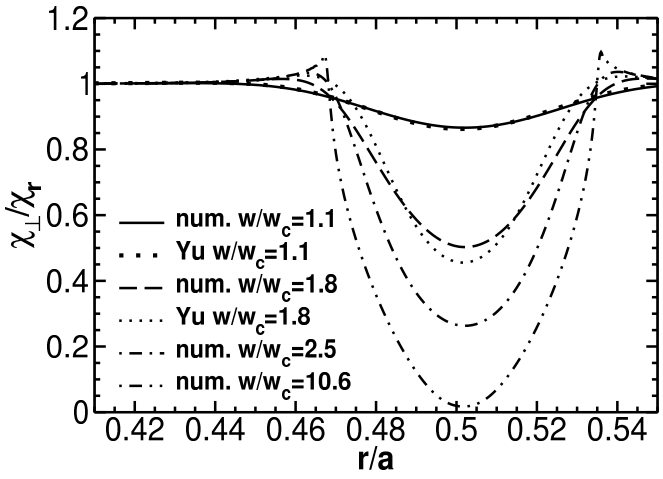

Figure 4: The inverse of the radial heat diffusivity χ_r normalized to $\chi_\perp$ at a $4/3$ magnetic island with $w = 0.068a$. For the first two cases, an analytical formula by Yu is plotted as well [2]. Although we are using it outside the range it was derived for ($w/w_c \ll 1$), the formula shows very good agreement with the numerical results for $w/w_c = 1.1$ and reasonable agreement even for $w/w_c = 1.8$.

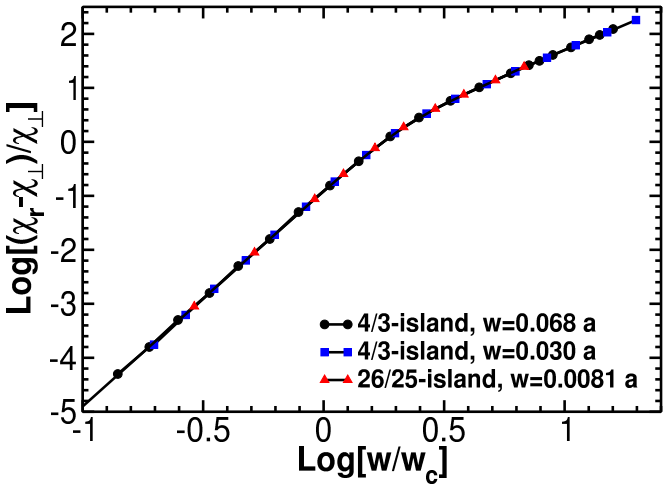

Figure 5: (Color online) The value of $\kappa = (\chi_r - \chi_\perp)/\chi_\perp$ at the resonant surface of single islands is plotted vs. w/w_c. Two regimes with $\kappa \propto (w/w_c)^4$ for small values of w/w_c and $\kappa \propto (w/w_c)^2$ for large values of w/w_c are found in agreement with previous work [1, 2]. The transition region is located between $w/w_c \approx 1$ and 4.5.

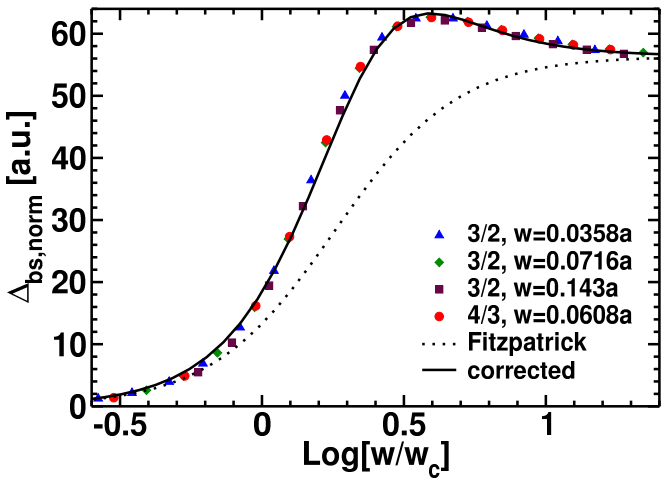

Figure 6: (Color online) Island drive caused by temperature perturbations. $3/2$ and $4/3$ island cases are plotted. Agreement with Fitzpatricks small and large island limits is found [1]. However, the matching between these limits, given in Eq. (4), underestimates the island drive for intermediate values of w/w_c significantly. With the correction factor we present in Eq. (5) applied, the numerical results are reproduced very well.

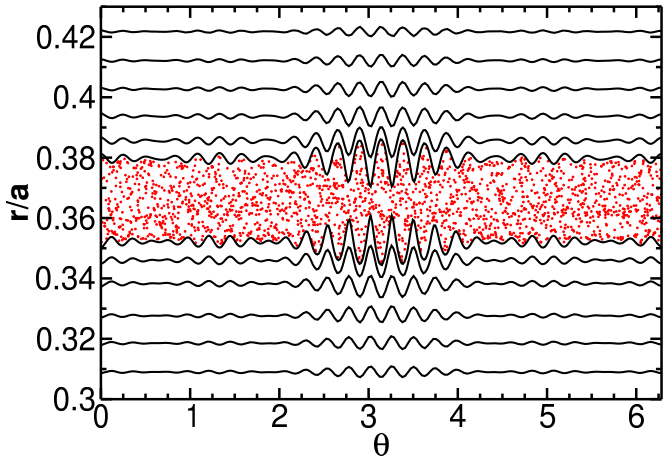

Figure 7: (Color online) Poincaré plot of the magnetic field structure of the highly ergodic case considered.

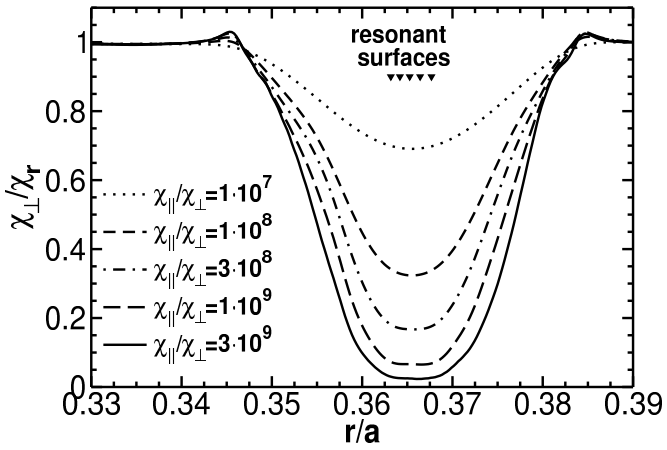

Figure 8: The inverse of the radial heat diffusivity χ_r normalized to $\chi_\perp$ at a highly ergodic layer produced by five magnetic perturbations with very similar helicities.

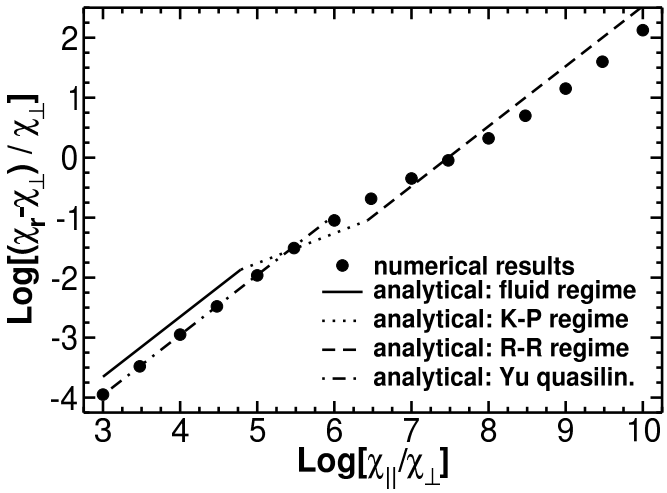

Figure 9: $\kappa = (\chi_r - \chi_\perp)/\chi_\perp$ at the center of the highly ergodic layer. Qualitative agreement between the analytically predicted and the numerically observed κ is found. However, the ranges of validity of the regimes and the absolute values do not coincide. Very good quantitative agreement is observed, when the fluid regime formula is corrected according to Yu [2].